The Resting Oxidized State of Small Laccase Analyzed with Paramagnetic NMR Spectroscopy

Rubin Dasgupta,[a] Karthick B. S. S. Gupta,[a] Huub J. M. de Groot,[a] and Marcellus Ubbink*[a]

The enzyme laccase catalyzes the reduction of dioxygen to water at the trinuclear copper center (TNC). The TNC comprises a type-3 (T3) and a type-2 (T2) copper site. The paramagnetic NMR spectrum of the small laccase from *Streptomyces coelicolor* (SLAC) without the substrate shows a mixture of two catalytic states, the resting oxidized (RO) state and the native intermediate (NI) state. An analysis of the resonances of the RO state is reported. In this state, hydrogen resonances only of the T3 copper ligands can be found, in the region of 12–22 ppm. Signals from all six histidine ligands are found and can be attributed to Hδ1, Hβ or backbone amide H^N nuclei. Two sequence-specific assignments are proposed on the basis of a second-coordination shell variant that also lacks the copper ion at the T1 site, SLAC–T1D/Q291E. This double mutant is found to be exclusively in the RO state, revealing a subtle balance between the RO and the NI states.

1. Introduction

The multicopper oxidase laccase can perform oxygen reduction with very little overpotential (~ 20 mV).[1] It comprises two active sites, a type-1 (T1) copper site to oxidize substrates and a trinuclear copper center (TNC) to reduce dioxygen to water. The TNC can be divided in a type-3 (T3) and a type-2 (T2) copper site. The T1 site is comprised of a single copper ion and is characterized by a strong absorbance at 600 nm due to the metal-sulfur charge transfer between the Cu(II) ion and a cysteine ligand.[2] The T3 site has two copper ions interacting via a hydroxide group, whereas the T2 site has a single copper ion in a trigonal planar geometry, coordinated by two histidine ligands and a water/OH⁻ group.[2] The current model of the reaction mechanism was previously described in detail.[3] In brief, the resting oxidized (RO) state is reduced to the fully reduced (FR) state by extracting four electrons from the substrates at the T1 site. The TNC has three cuprous ions in the FR state and can bind an oxygen molecule. Donation of two electrons from the TNC copper ions to the molecular oxygen leads to the formation of the peroxide intermediate (PI) state. At this stage the TNC needs one additional electron for complete oxygen reduction, which can be transferred from the reduced T1 site. In addition, for small laccases and human ceruloplasmin an electron can be transferred from the tyrosine

residue near the T2 site by forming a tyrosine radical.[4,5] Two electron transfers coupled with a single proton transfer convert the PI state to the native intermediate (NI) state in which the peroxide bond between the oxygen atoms is broken. After three protons transfers from the protein environment, two water molecules are released and the NI state is converted into the RO state without the substrates, or into the FR state, with the substrates in the environment.

However, somewhat in contrast with this standard model, the NMR spectrum of a small laccase from *Streptomyes coelicolor* (SLAC) showed that without substrate the enzyme exists as a mixture of RO and NI states with all the copper ions in the cupric form.[6,7] In the NI state, the T2 copper ion is coupled to the T3 copper ions via an oxygen atom (Figure S2b). The T2 copper ion is decoupled in the RO state (Figure S2a). The ¹H signals in the NMR spectrum of the RO state are less paramagnetically shifted (12 to 22 ppm) than those of the NI state (22 to 55 ppm).[6,7] The wild type protein (SLAC-wt, the native, holoprotein, with copper ions in all sites) is predominantly in the RO state, while the T1 site copper depleted mutant (SLAC–T1D) is mostly in the NI state.[6,7] Five chemical exchange processes ascribed to ring motions of histidine ligands coordinating the Cu(II) ions in both T3 and T2 sites were shown to be present for the NI state of SLAC–T1D.[7,8] Further characterization of these exchange processes requires sequence specific assignment of the resonances to the histidine ligand nuclei. The assignment of the resonances is complicated by the paramagnetic nature of the copper ions, resulting in line broadening and hyperfine shifted resonances (up to 60 ppm in SLAC). This makes it impossible to use standard multidimensional NMR experiments for the assignments. Mutations in the second shell of coordination were considered as a means to obtain assignments. Using such a mutation, two of the chemical exchange processes in the NI state could be assigned to the T2 site histidine ligands.[7] However, a detailed characterization of the RO state could not be done due to its low population in SLAC–T1D, resulting in the low S/N ratio of the corresponding resonances.[7]

[a] R. Dasgupta, Dr. K. B. S. S. Gupta, Prof. Dr. H. J. M. de Groot, Prof. Dr. M. Ubbink
Leiden Institute of Chemistry
Leiden University, Gorlaeus Laboratory
Einsteinweg 55, 2333 CC Leiden, The Netherlands
E-mail: m.ubbink@chem.leidenuniv.nl

ChemPhysChem

Articles
doi.org/10.1002/cphc.202100063

**Chemistry
Europe**
European Chemical
Societies Publishing

In the current study, SLAC-wt is studied to characterize the RO state. The electronic coupling between the two coppers leads to fast electronic relaxation, yielding observable signals even for nuclei close to the metals.[9–11] The signals from nuclei in the T2 site ligands are broadened beyond detection because of the longer electronic relaxation time of the isolated electron spin on the copper.[7,10,12] The resonances from the T1 site are expected to be shifted to different spectral regions, 500 to 700 ppm for cysteine Hβ, 30 to 50 ppm for histidine ring, <0 ppm for histidine Hβ and 12 to 20 ppm for other ligands.[13–15] The signals from the T3 site are observed in the region from 12 to 22 ppm.[6] They can be differentiated from the signals of the T1 site by their temperature dependence. T3 site signals have anti-Curie behavior, i.e. an increase in hyperfine coupling with increase in temperature, whereas the T1 site signals have Curie type behavior, i.e. a decrease in hyperfine coupling with increasing in temperature.[12] The temperature dependence of the resonances in the 12–22 ppm region observed for the RO state was reported[6] and later shown to have anti-Curie behavior. This suggests that all resonances in that region arise from the T3 site ligands.

Using paramagnetically tailored NMR experiments and a mutation near the T3 site, the sequence specific assignment of two T3 site histidine ligands is reported for the RO state. In addition, resonances corresponding to all the six histidine ligands of the T3 site could be found. Interestingly, the mutant enzyme is exclusively in the RO state, indicating that there is a subtle balance between the NI and RO states. Ultimately, assignment of the NMR resonances of nuclei at the heart of active site can lead to a better description of the TNC and aid in characterizing underlying motions, which may help to explain how laccases can so efficiently break the stable dioxygen bond.

2. Results and Discussion

2.1. RO State in SLAC-wt

The NMR spectra of the RO state comprise signals from the T3 site histidine ligands that span the spectral region between 12 and 22 ppm, while the NI state has signals from both the T3 and the T2 site histidine ligands in the spectral region between 22 and 55 ppm.[6,7] The spectrum of SLAC-wt reveals a mixture of the NI and the RO states, similar to SLAC–T1D.[6,7] The relative intensities of the signals in the RO and the NI spectral regions show that SLAC-wt is predominantly in the RO state, contrary to SLAC–T1D. A Gaussian deconvolution of the 1H spectral region between 10 and 22 ppm yields 14 resonances (Figure 1a). On the basis of 2D EXSY/NOESY (Figure 1b) and HMQC (Figure 1c) spectra, it can be concluded that some resonances derive from overlapping signals. The resonance at ~11 ppm is a super-position of proton signals (u0, c0, b0, e0 and x0), the resonances at ~16 ppm (u1 and b1) and 21.5 ppm (e2 and θ) are from two protons with strong overlap, and the resonance at ~19 ppm (b2, e1 and a2) is the summation of three proton signals. The cross-peaks between the resonances in the spectral region from 10 to 12 ppm have low S/N ratio and, therefore, we focus on

the resonances in the region of 12 to 22 ppm for further analysis (a1, x1, d0, x2, u1, b1, c1, d1, b2, e1, a2, d2, c2, θ and e2) (Figure 1b). These resonances show anti-Curie behavior, where the hyperfine coupling increases with temperature (Figure 1e), which is well in line with previous observations.[6] Using the coupled two-metal center model (equation S1), the singlet-triplet energy gap was estimated to be $2J = -560$ cm^{-1} with $S = 0$ being the ground state and the $S = 1$ the excited state. This value is within the range of the reported values for the RO state of laccases (-550 to -620 cm^{-1}).[6,7,16] Extrapolation of the fitted curves to infinite temperature yields the diamagnetic chemical shifts (δ_{dia}).[12,17,18] On the basis of BMRB statistics, resonances related to the Hδ1, Hβ and backbone amide H^N protons of the T3 histidine ligand are distinguished (Figure 1e, see also Experimental Procedures in the Supporting Information). Resonances e2, c2, d2, b2, c1 and a2 derive from Hδ1, with a globally fitted δ_{dia} of 10 ppm, in line with the BMRB average for the histidine ring Hδ1 of 9.5 ppm. The resonances e1, d1, b1 and u1 are from Hβ with a δ_{dia} of 3.3 ppm, matching the BMRB average of histidine Hβ of 3.2 ppm, while resonances a1, x2, d0 and x1 are attributed to backbone amide H^N with a δ_{dia} of 8.6 ppm with a BMRB average for the histidine backbone amide proton of 8.2 ppm. Assignments of resonances to nitrogen attached protons were validated by observation in a ^{15}N-^{1}H HMQC spectrum. Finally, an additional resonance θ is poorly resolved due to strong overlap with resonance c2.

The temperature dependence of the cross-peak intensities from the EXSY/NOESY spectrum shows that resonances x1 and x2 are in chemical exchange (Figure 1d), whereas other peaks are NOE cross peaks (a1a2, b1b2, c1c2, d0d2, d1d2 and e1e2). Cross peaks e1e2, d1d2 and b1b2 are the NOEs between the Hδ1 and Hβ protons, whereas cross peaks d0d2, and a1a2 are between the Hδ1 and backbone amide H^N protons. Cross peak c1c2 will be discussed further in the analyses of the double mutant SLAC–T1D/Q291E. Figure 1b shows that the resonances c, b, d and e have two cross peaks. The cross peaks e0e2, b0b2 and c0c2 could not be analyzed further due to their low S/N ratio but for resonance d NOE cross peaks are present between Hδ1 – Hβ and Hδ1 – backbone amide H^N protons (Figure 1b and 1e).

Analysis of the crystal structure (PDB 3cg8)[21] of *S. coelicolor* SLAC reveals that in His156 and His287 (numbering from the crystal structure 3cg8) the Hδ1 proton is close to both Hβ and a backbone amide H^N proton (Figure 2), which could give rise to the observed NOE cross peak pairs for the d resonances. The Hδ1 proton of His156 is at 2.65 Å from the nearest Hβ proton and at 3.13 Å from the backbone amide H^N of Asp157. In His287, the Hδ1 proton is at 2.53 Å from the closest Hβ proton and at 3.50 Å from the backbone amide H^N of Cys288 (Figure 2). According to previous studies the resonances of nuclei in ligands of the T1 site, including Cys288, are subject to Curie behavior, and the hyperfine coupling decreases with increasing temperature.[23] In contrast, resonance d0 shows an anti-Curie behavior (Figure 1e), which is generally observed for nuclei interacting with a coupled metal ion system.[12,17,18,23] This suggests that the resonance d can be assigned to His156, showing NOEs between the Hδ1 – Hβ and Hδ1 – Asp157 H^N.
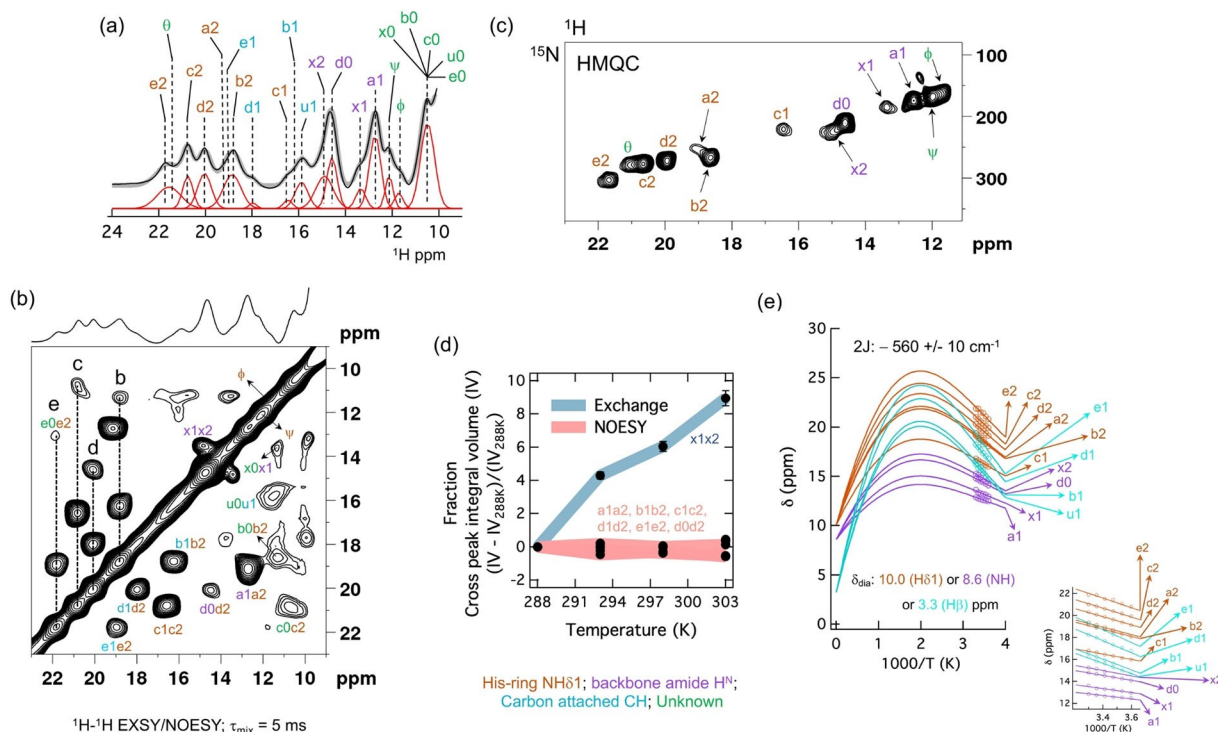
ChemPhysChem

Articles
doi.org/10.1002/cphc.202100063

Chemistry
Europe
European Chemical
Societies Publishing

Figure 1. NMR spectra of SLAC-wt. a) 1D WEFT[19,20] [1]H spectrum of the spectral region from 10 to 24 ppm corresponding to the RO state. The WEFT delay was set to 100 ms. Gaussian deconvolution is shown in red and the summation of the deconvoluted resonances is indicated with a solid grey trace. b) 2D [1]H-^{1}H EXSY/NOESY spectrum at 298 K with mixing time (τ_{mix}) of 5 ms. The 1D ^{1}H spectrum is shown on top of the spectrum. c) 2D [15]N-^{1}H HMQC spectrum. The delay for polarization transfer was set to 0.5 ms.[7] d) The temperature dependence of the fractional cross peak integrals to differentiate between the NOE and exchange cross peaks. e) Temperature dependence of the chemical shift of the resonances marked in panels (a), (b) and (c). The solid lines represent the fit using Equation S1. The 2 J value and the diamagnetic chemical shifts are shown. The inset shows an enlargement of the experimental region. The corresponding hyperfine coupling constants A (in MHz) are given in Table S3. The chemical shift values at different temperatures for each resonance in panel e is given in Table S4. The chemical shift values for resonances a2, x2, e1 and b1 were obtained from the temperature dependence of the cross peak in panel b. Color codes are given below panel d as brown for protons from the His-ring Hδ1, purple for the protons of the backbone amide H^N, cyan for the carbon attached protons and green for unknown. All spectra were recorded at 14 T.

The chemical shifts of the Hδ1, Hβ and Asp157 backbone amide H^N protons are 20, 18 and 14.5 ppm, with the paramagnetic shift contributions of about 10, 15 and 6 ppm, respectively. Interestingly, the paramagnetic contribution to the chemical shift of Hδ1 is less than for Hβ, although the former is four bonds away from the metal center, and the latter five. Perhaps this can be explained by (a) the higher electronegativity of nitrogen sequestering much electron density compared to carbon, resulting in less electron density on the nitrogen attached proton and (b) His156 Hδ1 having a strong hydrogen bond with the carbonyl CO of Asp157 that can result in an extended Nδ1-Hδ1 bond, thus further reducing the electron spin density on the proton. The shift of the H^N appears quite large for an FCS of a nucleus so many bonds away from the copper ion but it is noted that this is based on an estimate for the diamagnetic chemical shift of 8.6 ppm. Amide proton chemical shifts can vary widely. Also, a pseudo-contact shift could contribute to the observed shift.

Similar to the cross peak d0d2, a1a2 is also a NOE between a Hδ1 (a1, 12.68 ppm) and a backbone amide H^N proton (a2, 19.17 ppm). From the available crystal structures of small laccase, it is not possible to specifically assign it to any of the T3 histidine ligands. Cross peaks b1b2 and e1e2 can be from any

of the remaining five T3 histidine ligands. Overall, resonances a, b, d (1–2) and e represent signals from four of the six T3 site histidine ligands, with resonance d (1–2) assigned to His156 and d0 to Asp 157 H^N (Table S1). A two-site, slow chemical exchange is observed for a backbone amide H^N proton (resonances x1 and x2, Figure 1). Although it is paramagnetically shifted, there are no NOE cross peaks with other resonances from the T3 site histidine ligands. In the state corresponding to x1, a weak cross peak is observed with resonance x0 (Figure 1b). It remains unclear to which nuclei these signals can be assigned.

2.2. Comparison between SLAC-wt and SLAC-T1D

Similar to SLAC-wt, the NMR spectrum of SLAC–T1D shows a mixture of the RO and the NI states.[6,7] A strong response in the NI region (22 to 55 ppm) compared to the RO region (12 to 22 ppm) provides convincing evidence that SLAC–T1D is predominantly in the NI state (Figure 3a).[7] The proton resonances from the 1D ^{1}H WEFT spectra of the RO region in SLAC–T1D are not well resolved due to their low S/N ratio (Figure 3b). However, the RO spectral region in the 2D [1]H-^{1}H EXSY/NOESY spectra shows that the cross-peaks (a1a2, b1b2,

ChemPhysChem

Articles
doi.org/10.1002/cphc.202100063

Chemistry
Europe
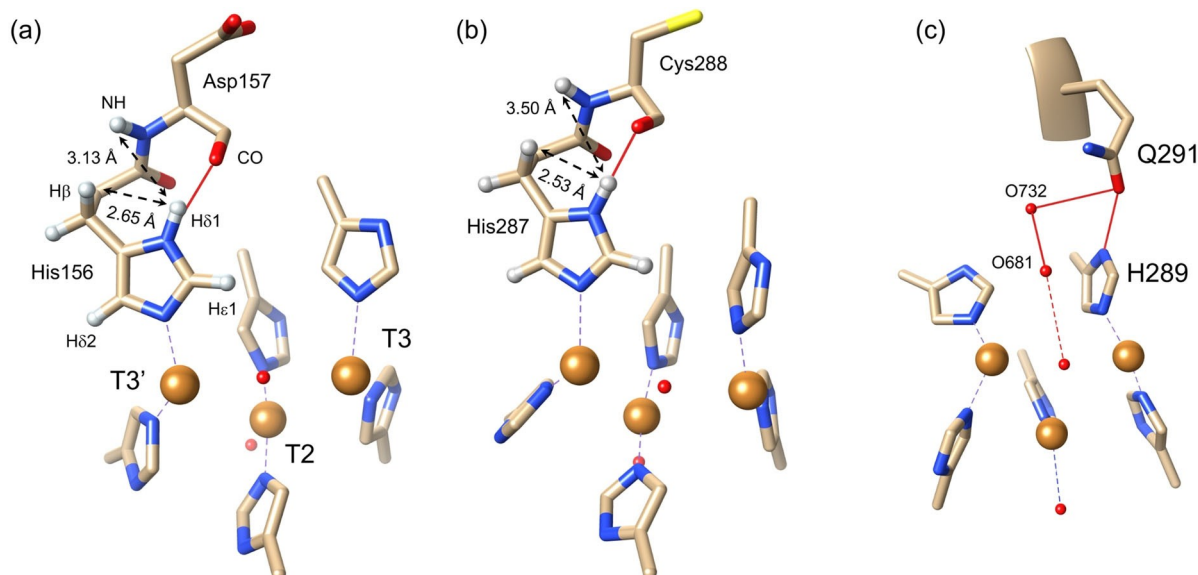European Chemical
Societies Publishing

Figure 2. Histidine ligands in the TNC of SLAC. Protons are shown near Hδ1 of His156 (a) and His287 (b) from the crystal structure of small laccase from *S. coelicolor* (PDB 3cg8).[21] Hydrogen bonds are shown as red lines. Amino acid residues are shown in golden sticks and copper ions as orange spheres. Distances between the Hδ1-Hβ and Hδ1-HN are shown as double-sided arrows. Protons of the histidine ring are marked in panel (a). The protons were modelled using the "AddH" algorithm as implemented in UCSF Chimera program[22] (for more details, see supporting information). His289 and 287 in panel a and His156 and 158 in panel (b) are not shown for clarity. c) Hydrogen bonds are shown from Gln291 Oε1 to His289 Nδ1 and the bound water molecule O732 (red sphere), which is part of the water channel (Figure S3). O732 is hydrogen bonded to the next water molecule O681 in the water channel. A possible hydrogen bond from O681 to the T3 site oxygen is shown as a red dashed line. His156, 158 and 102 are not shown for clarity.
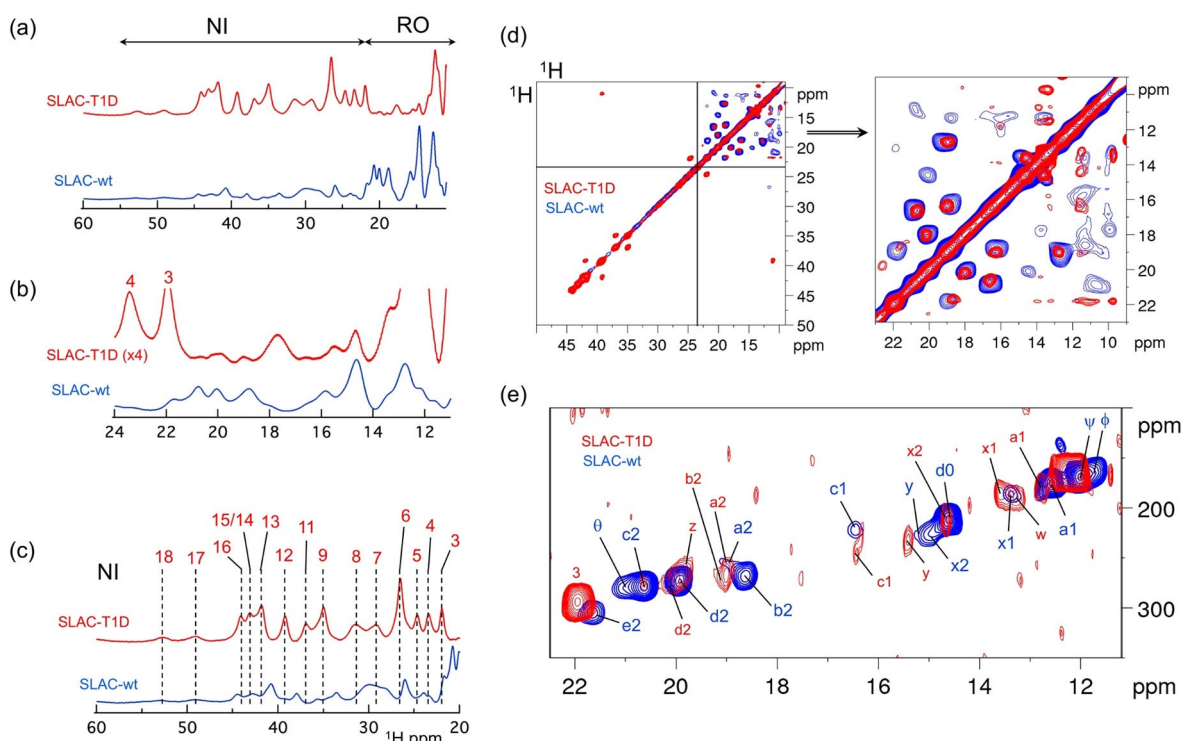

Figure 3. Comparison of SLAC–T1D and SLAC-wt. a) Overlaid 1D ^{1}H spectra of SLAC–T1D (red) and SLAC-wt (blue). The spectral regions for the NI (22 to 55 ppm) and the RO (12 to 22 ppm) states are marked. b) Expansion of the spectral region corresponding to the RO state where the spectral intensity of SLAC–T1D is multiplied by a factor 4. c) Expansion of the spectral region corresponding to the NI state. The chemical shifts are given in Table S2 of the supporting information. d) Overlaid ^{1}H-^{1}H EXSY/NOESY spectra of SLAC-wt and SLAC–T1D with an expansion of the spectral region 12 to 22 ppm. The resonance notations are in panel (b) of Figure 1. e) Overlaid ^{15}N-^{1}H HMQC spectra for the RO region.

ChemPhysChem

Articles
doi.org/10.1002/cphc.202100063

Chemistry
Europe
European Chemical
Societies Publishing

c1c2, d1d2, e1e2 and x1x2) are present in both SLAC–T1D and SLAC-wt (Figure 3d). Cross-peak d0d2 is not observed in SLAC–T1D due to its low S/N ratio. The ^{15}N-^{1}H HMQC spectrum is also similar between the two proteins, although some changes can be observed (Figure 3e). In SLAC–T1D, resonances a1, x1, y, b2 and d2 are shifted downfield, while resonance x2 is shifted upfield in the proton dimension and resonance c1 is shifted downfield in the nitrogen dimension. Additional resonances w and z are observed in SLAC–T1D. A downfield shifted resonance is correlated to an increase in the spin density on the nucleus and vice-versa for an upfield shifted resonance.[12,24] This suggests that in the RO state of SLAC–T1D, protons represented by resonances a1, x1, y, b2 and d2 have more spin density and x2 has less spin density compared to SLAC-wt. These changes can be attributed to the loss of the T1 copper in the T1D mutant, due to which the TNC is affected structurally and electronically.[6] Some structural change of the TNC is also suggested by the change in the singlet-triplet energy gap $2J = -560$ cm^{-1} for the RO state of SLAC-wt, which is $2J = -600$ cm^{-1} for SLAC–T1D,[7] because it was shown that a change in J is related to the change in the angle between the hydroxyl bridged T3 copper ions ($Cu^{2+}-OH^--Cu^{2+}$) and distance between the T3 coppers.[2,3]

The NI spectral region (22 to 55 ppm) of the 1D ^{1}H WEFT spectrum shows a similar pattern for SLAC-wt and SLAC–T1D. However, the resonances are broader for the SLAC-wt (Figure 3c). The resonances in SLAC–T1D are mostly downfield shifted compared to SLAC-wt, except for resonance 16, which is upfield shifted (Table S2). For resonances 17 and 18 the variations in chemical shift are small compared to their large linewidth. In summary, resonances from RO and NI states can be observed for both SLAC-wt and SLAC–T1D proteins, consistent with the previous observations.[6,7]

2.3. Analysis of SLAC-T1D/Q291E

It was shown that a mutation in the second coordination shell can help in assigning the complex paramagnetic NMR spectra of the nuclei in the TNC.[7] Using the SLAC–T1D/Y108F double mutant, the chemical exchange pairs 13–12 and 16–18 of the NI state (Figure 3c) were assigned to Hδ1 of His102 and His234 in the T2 site, respectively.[7] Following this method, a residue near the T3 site, Gln29, was mutated to aid in further assignment of the TNC ligands. A double mutant variant SLAC–T1D/Q291E was made to remove the effects of the T1 site copper. Gln291 is located near the T3 site of the TNC and its side chain is oriented toward the water channel leading into the TNC (Figure S3). This water channel has been proposed to be the source of protons in the formation of waters from dioxygen.[21,25] Gln291 also forms a strong hydrogen bond with the Nδ1 of His289 (Figure 2c), a ligand in the T3 site.

The 1D ^{1}H NMR spectrum of the double mutant SLAC–T1D/Q291E is compared with those of SLAC–T1D and SLAC-wt in Figure 4a. The NMR spectrum of the double mutant SLAC–T1D/Y108F was reported to be a mixture of the NI and the RO states with the NI state being the most populated, similar to the

situation in SLAC–T1D.[7] The NMR spectrum of SLAC–T1D/Q291E shows the enzyme to be exclusively in the RO state, without any signals from the NI state (Figure 4a).

A gaussian deconvolution of the ^{1}H spectral region between 12 and 24 ppm shows 11 resonances (Figure 4b). The 2D ^{1}H-^{1}H EXSY/NOESY spectrum (Figure 4d) reveals that the resonance at ~14.5 ppm consists of two resonances, d0 and x2, and similarly, in the resonance at ~16.8 ppm c1' and b1 are overlaid. The signal at ~19 ppm consists of four overlapping resonances d1, b2, e1 and a2. The temperature dependencies of the proton chemical shifts can be fitted to a coupled two-metal center model (Equation S1) yielding $2J = -560$ cm^{-1}, which is same as for SLAC-wt (Figure 4e and 1e). The resonances could not be specifically assigned to His Hδ1, Hβ and backbone amide H^N protons from this temperature dependency due to substantial signal overlap (Figure 4b). However, the similarity between the spectra of SLAC–T1D/Q291E and SLAC-wt (Figure 5a) indicates comparable assignments.

Overlaid NMR spectra of SLAC-wt and SLAC–T1D/Q291E reveal the changes in the RO state of the protein due to the Q291E mutation. The ^{1}H resonances for SLAC–T1D/Q291E are broader than for SLAC-wt (Figure 5a). Chemical shift perturbations are clear from the 2D ^{1}H-^{1}H EXSY/NOESY spectra, showing that resonances b2, c2, d0, d2, e2, x1 and x2 are downfield shifted, while resonance c1 is upfield shifted and resonance a1 is unperturbed (Figure panels 5b and 5d). Most of the resonances are downfield shifted, suggesting that the Q291E mutation leads to an increase in the spin density delocalization over the ligands in the TNC. It is of interest to note the ^{1}H-^{1}H cross peak c1c2 in SLAC-wt and c1'c2 in SLAC–T1D/Q291E. In the 2D ^{15}N-^{1}H HMQC, the resonance assigned as c1 in SLAC-wt is upfield shifted in the proton dimension and downfield shifted in the nitrogen dimension in the equivalent spectrum of SLAC–T1D/Q291E (Figure 5c). However, in the EXSY/NOESY spectrum the cross peak for c1c2 moves slightly downfield in the c1 dimension (Figure 5b). This cross-peak was assigned as c1'c2 in SLAC–T1D/Q291E and since c1' is suppressed in the HMQC data compared to the EXSY/NOESY spectrum it can be attributed to a carbon attached proton (Figure 4c and d). Most probably the resonances c1 and c1' overlap for SLAC-wt (Figure 1b and 5b), whereas in the spectrum of SLAC–T1D/Q291E they can be distinguished (Figure 5c). Resonances c1 and c1' may well belong to different histidine ligands. The temperature dependence of the chemical shift showed that resonance c1 derives from a Hδ1 nucleus. The resonance c2 also derives from a Hδ1 nucleus and because c1' can be attributed to a carbon attached hydrogen, the c1'c2 cross-peak is likely to represent another Hδ1-Hβ NOE from one of the T3 His ligands.

The chemical shift perturbations between SLAC–T1D/Q291E and SLAC-wt show that the strongest perturbation is for the resonance c1. Since Gln291 has a strong hydrogen bond with His289 (Figure 2c), the Q291E mutation can have a pronounced effect on the chemical shift of its Nδ1 and Hδ1 nuclei. Due to the negative charge, Glu291 is likely to have a stronger hydrogen bond with the Hδ1 of His289, increasing the N–H bond length and reducing the spin density on the proton while
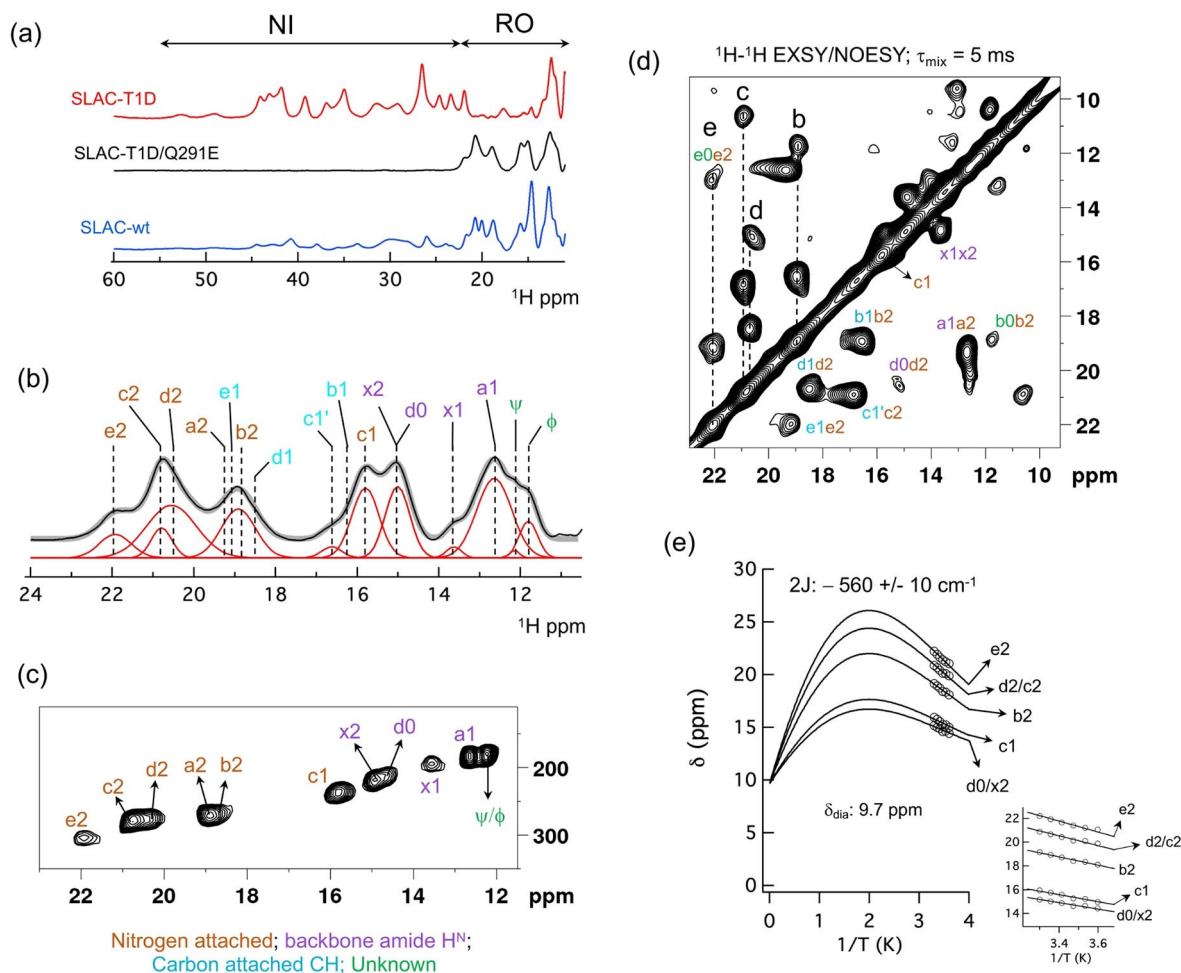
ChemPhysChem

Articles
doi.org/10.1002/cphc.202100063

**Chemistry
Europe**

European Chemical
Societies Publishing

Figure 4. NMR spectra of SLAC–T1D/Q291E. a) 1D ^{1}H spectra of SLAC–T1D (red), SLAC–T1D/Q291E (black) and SLAC-wt (blue). The spectral regions for the NI and the RO states are denoted. b) 1D ^{1}H spectrum of SLAC–T1D/Q291E in the spectral region from 11 to 24 ppm. A Gaussian deconvolution is shown in red and the summation of the deconvoluted resonances is shown as a solid grey trace. c) ^{15}N-^{1}H HMQC spectrum and d) ^{1}H-^{1}H EXSY/NOESY spectrum of SLAC–T1D/Q291E for the ^{1}H spectral region of the RO state. e) Temperature dependence of the resonances marked in panel (b). The solid line is the fit to Equation S1 (for more details see the experimental procedures in the supporting information). The inset shows an enlargement of the data region. The $2J$ and the diamagnetic chemical shifts are shown. The corresponding hyperfine coupling constants A (in MHz) are given in Table S3. The chemical shifts at different temperatures for each resonance in panel (e) are given in Table S5. The color code, assignments and the acquisition parameters are the same as in Figure 1.

increasing it on the nitrogen. This will result in an upfield shift for the proton and a downfield shift for nitrogen, in line with the observation in the HMQC spectrum (Figure 5c). Therefore, we propose that resonance c1 is from Hδ1 of His289 in the T3 site.

3. Conclusions

The NMR spectrum of SLAC-wt is a mixture of the RO and the NI states, and the intensity profile shows that the RO state is most populated. Paramagnetically tailored NMR experiments and the double mutant SLAC–T1D/Q291E helped to provide residue specific assignments for the Hδ1 nuclei of all the six histidine ligands of the T3 site (a2, b2, c1, c2, d2 and e2). The resonances d1 and d2 are assigned to His156 Hβ and Hδ1, respectively, d0 to Asp 157 H^N and resonance c1 is assigned to His289 Hδ1.

Cross peaks in the ^{1}H spectral region of 10–12 ppm could not be analyzed due to their low S/N ratio. Some of the cross peaks (b0b2, c0c2 and u0u1) are associated with resonances assigned to the T3 histidine ligands. Assuming that b0, c0 and u0 arise from the backbone amide H^N protons, cross peaks b0b2 and c0c2 might be NOEs between the His Hδ1 (b2 and c2) and backbone amide protons (b0 and c0). Cross peak u0u1 may be a NOE between a Hβ and a H^N.

Our previous work on SLAC showed the presence of five chemical exchange processes in the NI state involving Hδ1 protons and attributed to His ring motions.[7,8] In the RO state, these exchange processes are not observed. Perhaps the exchange is still present but not visible because the lower spin density on nuclei causes smaller FCS. For the NI state, the differences in chemical shift between the states represent ~10% of the FCS. The differences in chemical shift between the different states may be too small in the RO state to result in
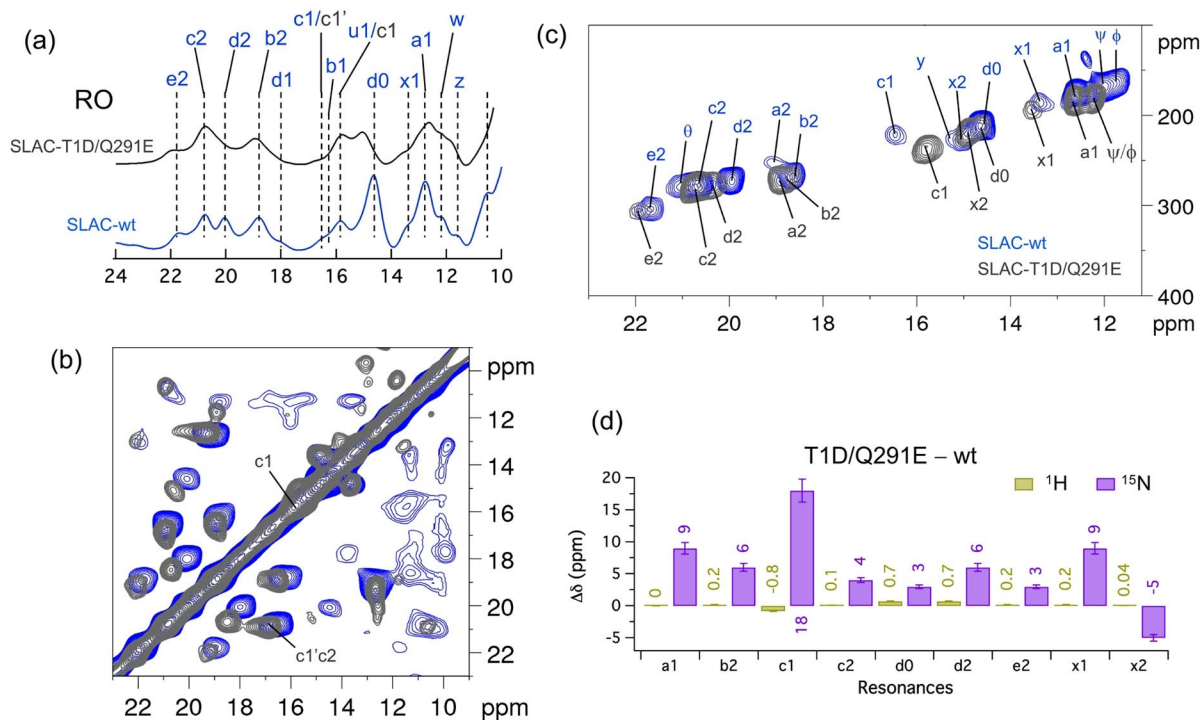
ChemPhysChem

Articles
doi.org/10.1002/cphc.202100063

Chemistry Europe
European Chemical
Societies Publishing

Figure 5. Comparison of SLAC–T1D/Q291E and SLAC-wt. Overlaid 1D ^{1}H NMR spectra (a), 2D ^{1}H-^{1}H EXSY/NOESY with the resonances c1, c1', and c2 marked (b), and ^{15}N-^{1}H HMQC with all the resonances marked (c) of SLAC–T1D/Q291E (black) and SLAC-wt (blue) of the spectral region 10 to 23 ppm. d) Chemical shift perturbations as the difference in chemical shift between SLAC–T1D/Q291E and SLAC-wt.

observable exchange peaks. Alternatively, the RO state may be more rigid, slowing down His ring motions sufficiently to bring the exchange rate outside the window that results in exchange cross peaks (80–200 s^{-1}). For the RO state, one exchange process was observed, between signals x1 and x2. However, these resonances do not derive from Hδ1 but from a shifted backbone amide signal. It provides evidence that some motion is occurring in the RO state as well, but we have not been able to assign it to a particular nucleus. We expect that the use of second coordination shell mutations can allow further assignment of the paramagnetic NMR signals from the TNC, providing spectroscopic probes that can help to understand how motions of the histidine ligands assist in progressing rapidly through the consecutive steps of the catalytic cycle.

Acknowledgements

Conflict of Interest

The authors declare no conflict of interest.

[1] N. Mano, V. Soukharev, A. Heller, *J. Phys. Chem. B* **2006**, *110*, 11180–11187.
[2] E. I. Solomon, D. E. Heppner, E. M. Johnston, J. W. Ginsbach, J. Cirera, M. Qayyum, M. T. Kieber-Emmons, C. H. Kjaergaard, R. G. Hadt, L. Tian, *Chem. Rev.* **2014**, *114*, 3659–3853.
[3] E. I. Solomon, A. J. Augustine, J. Yoon, *Dalton Trans.* **2008**, 3921–3932.
[4] A. Gupta, I. Nederlof, S. Sottini, A. W. J. W. Tepper, E. J. J. Groenen, E. A. J. Thomassen, G. W. Canters, *J. Am. Chem. Soc.* **2012**, *134*, 18213–18216.
[5] S. Tian, S. M. Jones, E. I. Solomon, *ACS Cent. Sci.* **2020**, DOI 10.1021/acscentsci.0c00953.
[6] M. C. Machczynski, J. T. Babicz, *J. Inorg. Biochem.* **2016**, *159*, 62–69.
[7] R. Dasgupta, K. B. S. S. Gupta, H. J. M. de Groot, M. Ubbink, *Magnetic Resonance Discussions* **2020**, 1–13.
[8] R. Dasgupta, K. B. S. S. Gupta, F. Nami, H. J. M. de Groot, G. W. Canters, E. J. J. Groenen, M. Ubbink, *Biophys. J.* **2020**, *119*, 9–14.
[9] L. Bubacco, J. Salgado, A. W. J. W. Tepper, E. Vijgenboom, G. W. Canters, *FEBS Lett.* **1999**, *442*, 215–220.
[10] N. N. Murthy, K. D. Karlin, I. Bertini, C. Luchinat, *J. Am. Chem. Soc.* **1997**, *119*, 2156–2162.
[11] M. Maekawa, S. Kitagawa, M. Munakata, H. Masuda, *Inorg. Chem.* **1989**, *28*, 1904–1909.
[12] I. Bertini, C. Luchinat, G. Parigi, E. Ravera, *NMR of Paramagnetic Molecules: Applications to Metallobiomolecules and Models*, Elsevier, Amsterdam, **2017**.
[13] A. P. Kalverda, J. Salgado, C. Dennison, G. W. Canters, *Biochemistry* **1996**, *35*, 3085–3092.
[14] G. W. Canters, H. A. O. Hill, N. A. Kitchen, E. T. Adman, *Eur. J. Biochem.* **1984**, *138*, 141–152.
[15] I. Bertini, S. Ciurli, A. Dikiy, R. Gasanov, C. Luchinat, G. Martini, N. Safarov, *J. Am. Chem. Soc.* **1999**, *121*, 2037–2046.

[16] L. Quintanar, J. Yoon, C. P. Aznar, A. E. Palmer, K. K. Andersson, R. D. Britt, E. I. Solomon, *J. Am. Chem. Soc.* **2005**, *127*, 13832–13845.

[17] I. Bertini, C. Luchinat, L. Messori, M. Vasak, *J. Am. Chem. Soc.* **1989**, *111*, 7300–7303.

[18] L. Banci, I. Bertini, C. Luchinat, in *Bioinorg. Chem.*, Springer, Berlin, Heidelberg, **1990**, pp. 113–136.

[19] S. L. Patt, B. D. Sykes, *J. Chem. Phys.* **1972**, *56*, 3182–3184.

[20] I. Bertini, C. Luchinat, G. Parigi, R. Pierattelli, *ChemBioChem* **2005**, *6*, 1536–1549.

[21] T. Skálová, J. Dohnálek, L. H. Østergaard, P. R. Østergaard, P. Kolenko, J. Dušková, A. Štěpánková, J. Hašek, *J. Mol. Biol.* **2009**, *385*, 1165–1178.

[22] E. F. Pettersen, T. D. Goddard, C. C. Huang, G. S. Couch, D. M. Greenblatt, E. C. Meng, T. E. Ferrin, *J. Comput. Chem.* **2004**, *25*, 1605–1612.

[23] L. Banci, I. Bertini, C. Luchinat, R. Pierattelli, N. V. Shokhirev, F. A. Walker, *J. Am. Chem. Soc.* **1998**, *120*, 8472–8479.

[24] I. Bertini, C. Luchinat, G. Parigi, *Prog. Nucl. Magn. Reson. Spectrosc.* **2002**, *40*, 249–273.

[25] A. Gabdulkhakov, I. Kolyadenko, O. Kostareva, A. Mikhaylina, P. Oliveira, P. Tamagnini, A. Lisov, S. Tishchenko, *Int. J. Mol. Sci.* **2019**, *20*, 3184.